Research Article

Sabah Ahmed Al-Zahrani, Ramesa Shafi Bhat*, Sarah A. Al Rashed, Amer Mahmood, Ahmed Al Fahad, Ghadah Alamro, Jamilah Almusallam, Roua Al Subki, Raha Orfali, and Sooad Al Daihan

Green-synthesized silver nanoparticles with aqueous extract of green algae *Chaetomorpha ligustica* and its anticancer potential

https://doi.org/10.1515/gps-2021-0067
received July 08, 2021; accepted October 06, 2021

Abstract: Marine green algae are rich in various bioactive components with known anticancer activity. Some anticancer drugs present in green algae are in clinical trials nowadays. Algae-mediated silver nanoparticles (AgNPs) have been of a great interest in cancer treatment due to their unique physico-chemical properties. In this study, we evaluate the anticancer efficiency of marine alga *Chaetomorpha ligustica* collected from the Arabian Gulf against colon cancer cell lines HT29 and HCT116. The anticancer potential of biosynthesized AgNPs from *C. ligustica* extract is also reported. Fourier transform infrared (FTIR) spectroscopy and gas chromatography-mass spectrometry analyses were used to identify the phytoconstituents present in algae extract. The synthesized AgNPs were confirmed via UV-Vis spectroscopy, whereas their morphology and stability were recorded by transmission electron microscopy (TEM), zeta potential, and zetasizer. We recorded absorption peak at 420 nm; TEM images showed an average size of 8.8 nm, whereas zeta potential and zetasizer study showed aggregation of nanoparticles. FTIR spectroscopy peaks of *C. ligustica* AgNPs were a little different from those of the *C. ligustica* extract. Both extracts showed cytotoxicity against cancer cell lines in a dose-dependent manner, but nanoparticles were found to be more toxic than algae extract. HT29 was found to be more sensitive than HCT116. For the first time, species of *C. ligustica* have been used and reported for the synthesis of nanoparticles. *C. ligustica* and its biogenic nanoparticles need to be scaled up for many biomedical applications especially in cancer research.

Keywords: *Chaetomorpha ligustica*, green algae, silver nanoparticles, cytotoxicity

*** Corresponding author: Ramesa Shafi Bhat,** Biochemistry Department, College of Science, King Saud University, Riyadh, Saudi Arabia, e-mail: rbhat@ksu.edu.sa
Sabah Ahmed Al-Zahrani, Ghadah Alamro, Jamilah Almusallam, Sooad Al Daihan: Biochemistry Department, College of Science, King Saud University, Riyadh, Saudi Arabia
Sarah A. Al Rashed: Department of Botany and Microbiology, King Saud University, Riyadh, Saudi Arabia
Amer Mahmood: Department of Anatomy, King Saud University, King Khalid University Hospital, Riyadh, Saudi Arabia
Ahmed Al Fahad: National Center for Pharmaceutical Technology Life Science & Environment Research Institute, King Abdulaziz City for Science and Technology, Riyadh, Saudi Arabia
Roua Al Subki: Clinical Laboratory Sciences Department, College of Applied Medical Sciences, King Saud University, Riyadh, Saudi Arabia
Raha Orfali: Department of Pharmacology, College of Pharmacy, King Saud University, Riyadh, Saudi Arabia

1 Introduction

Herbal medicine in the form of extracts, powders, brews, or gels has been used to treat various ailments both in humans and animals [1]. Primary health care through herbal medicine is a very common practice in developed and in developing countries [2]. Cancer is a major cause of death in humans, and colorectal cancer is the third most diagnosed form of this disease all over the world [3]. A large number of preventive therapeutic studies are going on all over the world to find a way to ameliorate cancer incidence and/or reduce cancer mortality in human populations [4]. An enhanced search for natural compounds that can help in preventing cancer is being explored keenly. Most of the herbal medicines are derived from plants, but some algae are being focused on due to their novel bioactive compounds [5]. Algae are heterogeneous organisms, existing as brown (*Phaeophyta*), red (*Rhodophyta*), and green (*Chlorophyta*) and are mainly divided as microalgae and macroalgae. Various bioactive metabolites with potent cytotoxicity against different kinds

of cancers are being explored from marine macroalgae or seaweeds [6]. Some recent studies reported many novel anticancer drugs present in seaweeds [7–10] and Kahalalide F, an antitumor marine drug, present in green algae are in clinical trials nowadays [11].

Chaetomorpha, one of the genera of green algae, are macroscopic unbranched filaments of cylindrical-shaped cells and are mostly found in the intertidal zone of the seas. The *Chaetomorpha* sp. are a rich source of antioxidants and possess drug properties against various human diseases [12]. Currently, many biomedical compounds present in *Chaetomorpha* sp. are being explored for various cancer therapeutic treatments such as chemo-protective agents, anticancer and drug-delivery systems [13,14]. *Chaetomorpha* sp. are a rich source of proteins, carbohydrates, fatty acids, pigments, and secondary metabolites, such as phenols, sulfated polysaccharides, and halogenated compounds [15]. Besides being strong antitumor, antiviral, antibacterial, and cytotoxic agents, these compounds have the ability to convert metal ions into metal nanoparticles due to their reducing and capping properties [16].

Biological methods of preparing nanoparticles are less toxic with low cost as compared to physical or chemical methods [17]. Being rich in bioactive compounds, plants are preferred for the green synthesis of metallic nanoparticles [18]. Plant-mediated metal nanoparticles are either synthesized intracellular, that is, inside plant tissue or extracellular by using plant extract [19,20]. Biomolecules present in plants significantly influence the quality and quantity of metal nanoparticles and thus determine their application approach. Due to unique surface chemistry, charge, energy, and spatial dimensions, metal nanoparticles offer outstanding applications in many fields of biomedicine [21]. They are widely used in drug-delivery systems, *in vitro* diagnostic tests, as biosensors and antimicrobial and anticancer agents [22,23]. Metal nanostructures are used as cargo molecules for imaging and gene delivery in many anticancer therapies. Metal nanoparticles can hinder some signal cascades that are responsible for the development and pathogenesis of tumors. Biogenic metal nanoparticles are found to be more cytotoxic against human cancer cells as compared to normal cells [22].

Algae-mediated silver nanoparticles (AgNPs) have been of a great interest in biomedicine especially cancer treatment and for targeted delivery of various anticancerous drugs [16]. This study examined the *in vitro* anticancer potential of marine alga *Chaetomorpha ligustica* collected from the Arabian Gulf against two colon cancer cell lines HCT116 and HT 29. Biologically synthesized AgNPs mediated by water extract of *C. ligustica* were also reported in this study.

2 Materials and methods

2.1 Collection of algae

The green algae, *C. ligustica*, was collected from the shore of the Arabian Gulf. It was washed properly with distilled water and then shade dried at room temperature. Once dry, it was powdered in an electric blender. One gram of powder was dissolved in 100 mL of sterile autoclaved water and left on a magnetic stirrer for 48 h at 4°C. Then, the mixture was filtered by using Whitman No. 1 filter paper. The obtained extract was stored at −80°C for further experiments.

2.2 Fourier transformed infrared (FTIR)

Perkin Elmer FTIR-Spectrometer Spectrum (Spectrum BX, USA) was used to identify the functional groups present in algae extract. FTIR was measured in the range from 4,400 to 400 cm^{-1}. The spectra (16 scans per spectrum) were collected with a spectral resolution of 16.0 cm^{-1} with an interval of 2.0 cm^{-1}.

2.3 Gas chromatography-mass spectrometry (GC-MS)

The phytochemical analysis of hexane extract of *C. ligustica* was accomplished by GC-MS analysis. GC Column TRACE™ TR-35MS (Thermo Fisher Scientific, USA) with the film thickness of 0.25 µm, length of 30 m, and diameter of 0.25 mm was used. The carrier gas was helium (99.9999% purity) at a flow rate of 1.2 mL·min^{-1}. The injector temperature was set to 250°C. The injection mode was split less, and the injection volume was 1.0 µL. The GC column temperature was programed as an initial temperature of 60°C, held for 3 min, increased at a rate of 10°C·min^{-1} to 300°C, and held for 5 min.

2.4 Biogenically synthesized AgNPs from *C. ligustica* extract

AgNPs were synthesized by dissolving silver nitrate ($AgNO_3$) solution in *C. ligustica* extract with the concentration of 5 mM $AgNO_3$ in the mixture. The reduction of silver ions to AgNPs was observed by a color change from light green to dark brown.

2.5 Characterization of biogenically synthesized AgNPs

Prepared nanoparticles were characterized as described below before treating the cells.

2.5.1 UV-Vis spectrophotometer

Prepared nanoparticles were initially confirmed by observing a UV-Visible spectrophotometer from 300 to 600 nm with a peak at 420 nm by using the UV-Vis spectrophotometer (Thermo Scientific 1500, USA).

2.5.2 Transmission electron microscopy (TEM)

The shape and size of the nanoparticles were determined by using TEM. A grid coated with copper was used to place the silver nanoparticle sample to be imaged under TEM (JEOL JEM-1400 Plus, Japan).

2.5.3 Zetasizer and zeta potential

The average size of nanoparticles was recorded by Zetasizer Nano Series ZS (ZEN3600), UK by using the technique of dynamic light scattering (DLS) and zeta potential by electrophoretic light scattering (ELS).

2.6 Cell lines

In this study, two types of colon cancer cell lines, HT 29 and HCT116, were included. According to ATCC, the Global Bio-resource Center, HCT116 is derived from carcinoma-primary and HT29 adenocarcinoma-primary.

2.7 Cell treatment

2.7.1 Cell viability

Cell lines were divided into three groups depending upon the treatment: control or untreated, *C. ligustica* extract (10, 20, 50, and 100 µg) treated, and *C. ligustica* AgNPs (10, 20, 50, and 100 µg) treated for 48 h.

2.7.2 Expression level of genes

Cells were divided into three groups as control or untreated, *C. ligustica* extract (50% cytotoxic) treated, and *C. ligustica* AgNPs (50% cytotoxic) treated for 24 h.

2.8 Determination of cell viability

Cell viability was measured by MTT (3-(4,5-dimethylthiazol-2-yl)-2,5-diphenyltetrazolium bromide) assay. Absorbance was measured at 490 nm using a scanning microliter-well spectrophotometer. The color intensity is correlated with the number of healthy living cells.

2.9 Determining the expressional level of ataxia telangiectasia mutated (ATM), ataxia telangiectasia and Rad3 related (ATR), checkpoint kinase (CHK1), and CHK2 using RT-PCR

2.9.1 Nucleic acid isolation

After treatment, RNA samples were extracted from two different colon cancer cell lines by using an RNeasy mini kit (Qiagen, DE). All extractions were performed following the manufacturer's procedure.

2.9.2 cDNA preparation

cDNA synthesis was performed by reverse transcription of total purified by using the high-capacity cDNA reverse transcription kit (Applied Biosystems, USA). The cDNA synthesis was performed according to the manufacturer's procedure. The obtained cDNA samples were stored at –20°C.

2.9.3 Expressional level of genes

Power SYBR® Green PCR Master Mix 2X from Applied Biosystems® (Life Technologies, USA) was used to perform quantitative real-time PCR. All colon cancer cell lines were analyzed in triplicate, and gene expression was normalized to glyceraldehyde 3-phosphate dehydrogenase (GAPDH); a nontemplate negative control was included in each run to check background signal. Primer sequences and annealing temperature are listed in Table 1.

Table 1: Primer sequences of ATM, ATR, CHK1, CHK2, and GAPDH

Primer	Sequence	Annealing temperature (°C)
ATM	Forward: 5′-GCA GAT GAC CAA GAA TGC AA-3′ Reverse: 5′-GGC CTG CTG TAT GAG CAA AT-3′	60
ATR	Forward: 5′-GGGATGCCACTGCTTGTTATGAC-3′ Reverse: 5′-CTGTCCACTCGGACCTGTTAGC-3′	60
CHK1	Forward: 5′-CTTTGGCTTGGCAACAGT-3′ Reverse: 5′-CCAGTCAGAATACTCCTG-3′	60
CHK2	Forward: 5′-CTC GGG AGT CGG ATG TTG AG-3′ Reverse: 5′-CCAGTCAGAATACTCCTG-3′	57
GAPDH	Forward: 5′-GGTATCGTGGAAGGACTCATGAC-3′ Reverse: 5′-ATGCCAGTGAGCTTCCGTTCAGC-3′	60

2.10 Statistical analysis

Statistical analyses were carried out using GraphPad Prism® 9.0 statistical software (GraphPad Inc., USA) and Microsoft Excel®. An independent *t*-test was used to evaluate the difference in gene expression between the different stages of colon cancer cell lines and treated and untreated colon cancer cell lines. The level of significance used throughout was $p < 0.05$.

3 Results

3.1 FTIR of *C. ligustica* extracts

FTIR spectroscopy was measured for *C. ligustica* extract as shown in Figure 1. The 3403.66, 2924.81, and 2554.91 cm^{-1} absorption peaks were assigned for the OH bond of phenols, the N–H bond of amines, and S, O–H bond of carboxylic acid, respectively, for lipids. The 1707.76 cm^{-1} absorption

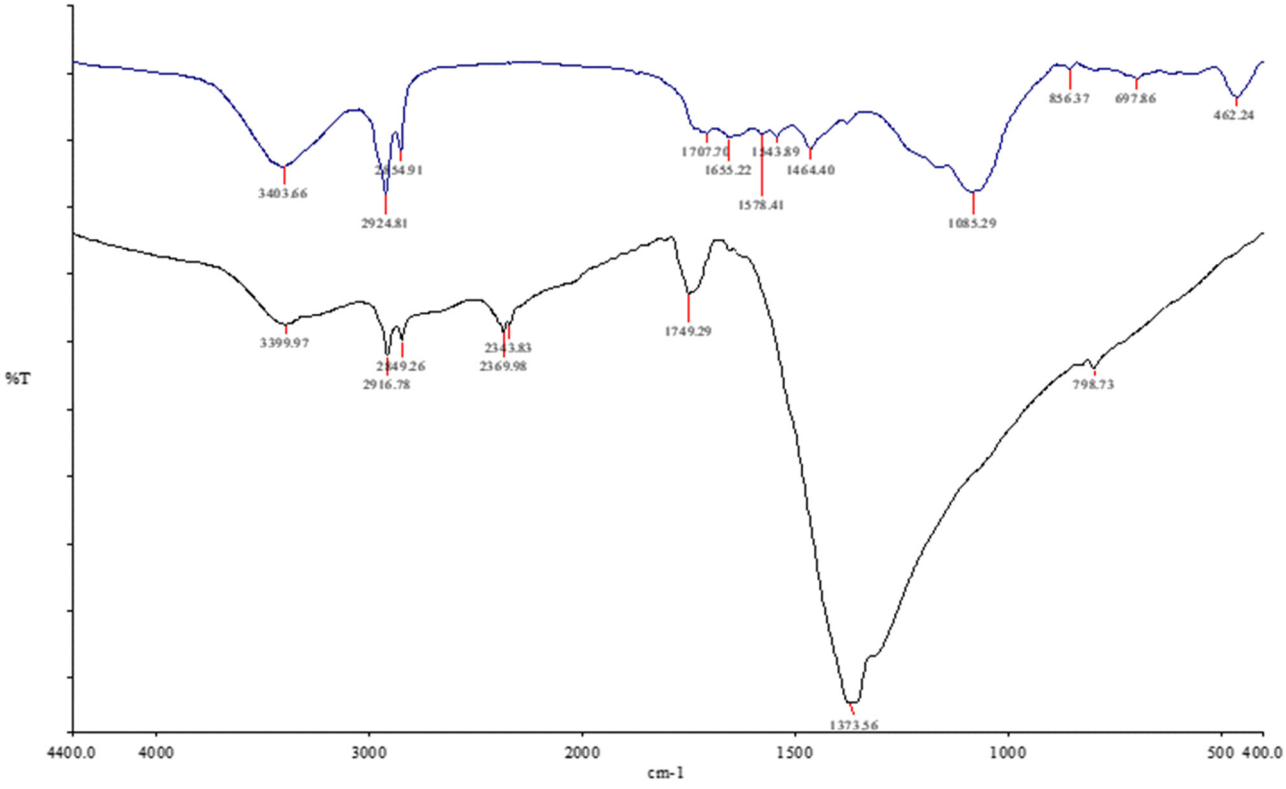

Figure 1: IR spectra of *C. ligustica* extract (blue color) and *C. ligustica* AgNPs (black color).

peak was assigned for the C═O stretch of ketone and C═C stretch of benzene; 1,655 cm^{-1} absorption peak was assigned for N–H, and 1578.41 and 1543.89 cm^{-1} absorption peaks were assigned for C–C stretch for amides in proteins. The 1464.40 cm^{-1} absorption peak was assigned for N–H bond (nitro compounds), C–O stretch (amides), C═C (benzenes), and C═O (ketones) in carbohydrates. 1085.29 for S═O stretch (sulfoxides), C–N stretch (amines), C–O stretch (esters, ether, alcohol), and ═C–H bend (alkenes). The 856.37 cm^{-1} absorption peak was assigned for C═C–H bend (alkenes) in pectin. The 697.86 and 462.24 cm^{-1} absorption peaks were assigned for C–N stretch (amines), ═C–H bend (benzene), and C–C stretch (chlorides) for cell wall components.

3.2 GC-MS analysis of *C. ligustica* extracts

GC-MS analysis of *C. ligustica* extracts leads to the identification of many compounds with anticancer properties. The components present in *C. ligustica* extract with anticancer properties detected by the GC-MS are shown in Figure 2. Antitumor compounds mainly detected in *C. ligustica* extract include methanone, propanoic acid, milbemycin B, eucalyptol, and fucoxanthin. Other than these cyclohexane; heptane; 2,4,6,8,10-tetradecapentaenoic acid; benzene; docosanoic acid; 1,2,3-propanetriyl ester; 3,8,12-tri-*O*-acetoxy-7-desoxyingol-7-one; trisiloxane; 12,15-octadecadiynoic acid; methyl ester; cyclopentasiloxane; decamethyl; cyclohexasiloxane; dodecamethyl; bicyclo[2.2.1]heptan-2-one; 1,7,7-trimethyl-cycloheptasiloxane; tetradecamethyl; benzaldehyde; 2,5-dimethyl; (3,4,trans-6-trimethyl-3-cyclohexenyl)formaldehyde 2,4-dinitrophenylhydrazone; D-homo-24-nor-17-oxachola-20,22-diene-3,16-dione; methyl glycocholate; 7,9-di-tert-butyl-1-oxaspiro(4,5)deca-6,9-diene-2,8-dione; ethyl isoallocholate; 7,8-epoxylanostan-11-ol; and 3-acetoxy were present in *C. ligustica* extracts.

3.3 Characterization of *C. ligustica* AgNPs

Figure 3a presents the UV spectra of *C. ligustica* AgNPs recorded at 3 h duration from the initiation of reaction between *C. ligustica* extract and $AgNO_3$ solution with a constant maximum absorption at 420 nm, which represents silver nanospheres. Results from TEM images showed the average size of 8.8 nm (Figure 3b); however, DLS analysis showed size as 1,800 nm (Figure 3c), indicating aggregation of nanoparticles. ELS analysis showed the zeta potential of 2.36 mV. FTIR spectroscopy result of *C. ligustica* AgNPs was a little different from that of the *C. ligustica* extract as some of the peaks belonging to functional groups of carbohydrate and proteins were not found as shown in Figure 1.

3.4 Cell viability

Results of cytotoxic effects of *C. ligustica* extract and *C. ligustica* AgNPs against human colon cancer cell lines HT29 and HCT116 after treatment are presented in Figure 4.

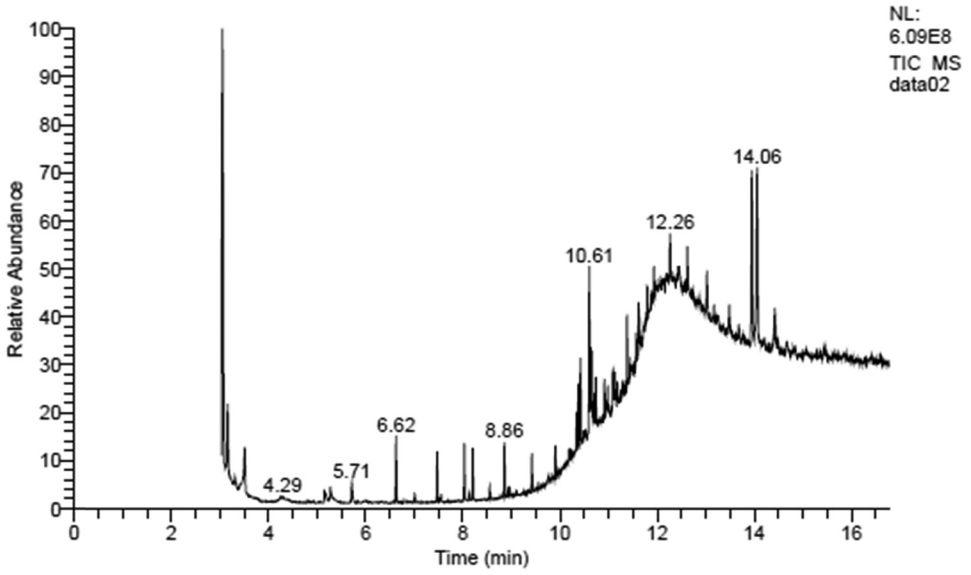

Figure 2: GC-MS analysis to detect the anticancer compound in *C. ligustica* extract.

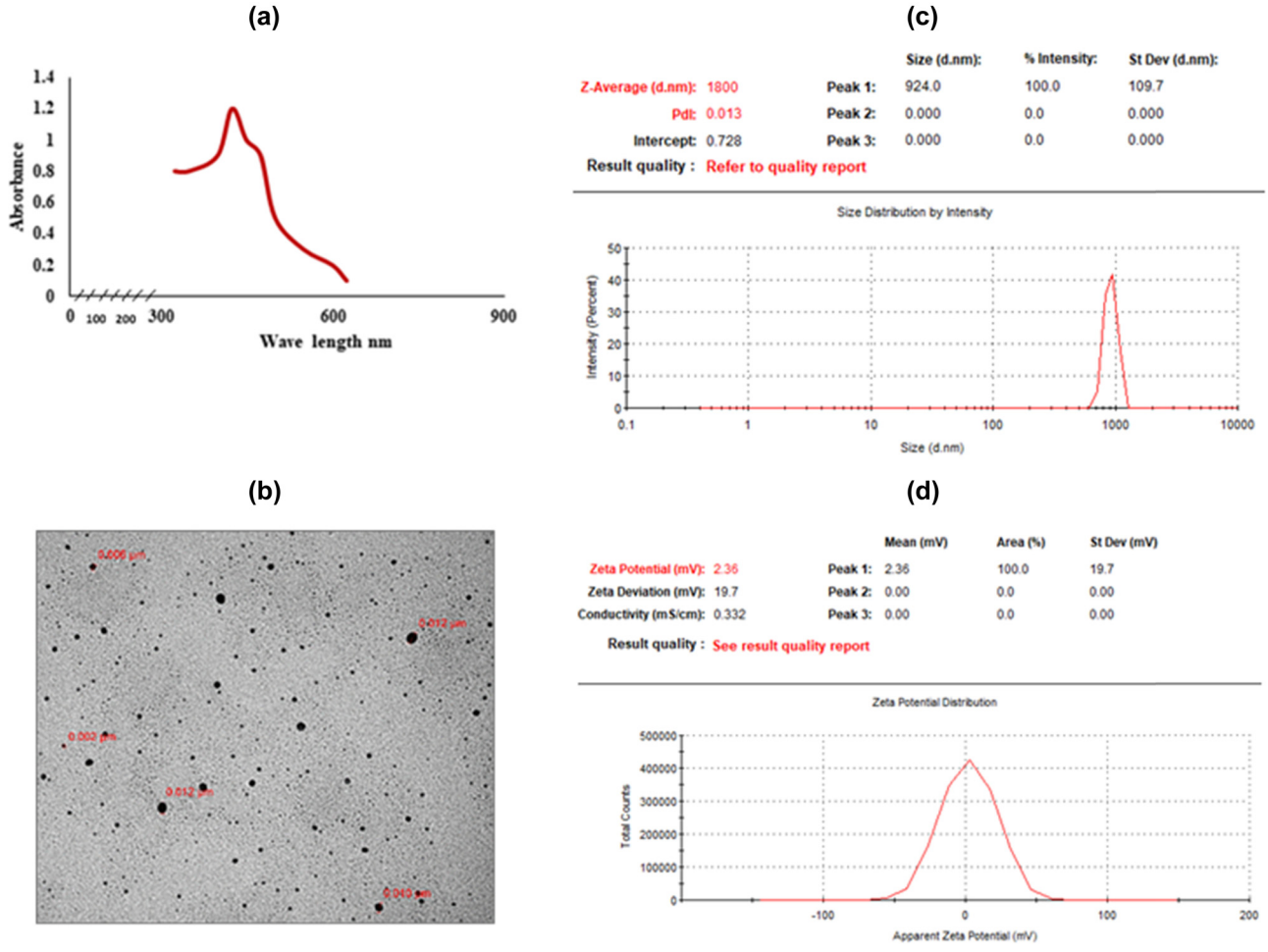

Figure 3: Characterization of biologically synthesized *C. ligustica* AgNPs: (a) UV-Vis spectra showing absorbance peak, (b) TEM micrograph, (c) zetasizer – DLS, and (d) zeta potential distribution – ELS.

C. ligustica extract was found more toxic at 10 μg·mL^{-1} as compared to *C. ligustica* AgNPs, but with the increase in concentration C. *ligustica* AgNPs showed higher cytotoxicity against both the cell lines.

3.5 Expressional level of ATM, ATR, CHK1, and CHK2 in cell lines treated with *C. ligustica* extract and *C. ligustica* AgNPs extract

As shown in Figure 5, the expression level of all the four genes (*ATM*, *ATR*, *CHK1*, and *CHK2*) was increased with treatment in HT29. In HCT116, the expression level of ATM was decreased with *C. ligustica* extract and AgNP treatment, but we found a slight increase in gene expression levels of other genes on treatment as shown in Figure 5.

4 Discussion

Green algae are being explored for drug properties for the fight against many diseases, including colorectal cancers, as they are found rich in many therapeutic compounds that can induce apoptosis through different molecular mechanisms [24,25]. The cytotoxic potential of various marine macroalgae against the growth of many kinds of cancer cell lines has been reported in the literature [25–29]. We explored both *C. ligustica* extract and *C. ligustica* AgNPs for cytotoxicity. FTIR and GC-MS analyses were used to identify the phytoconstituents present in algae extract.

4.1 FTIR of *C. ligustica* extracts

FTIR analysis is one of the most reliable and sensitive methods used by researchers to identify the biomolecules

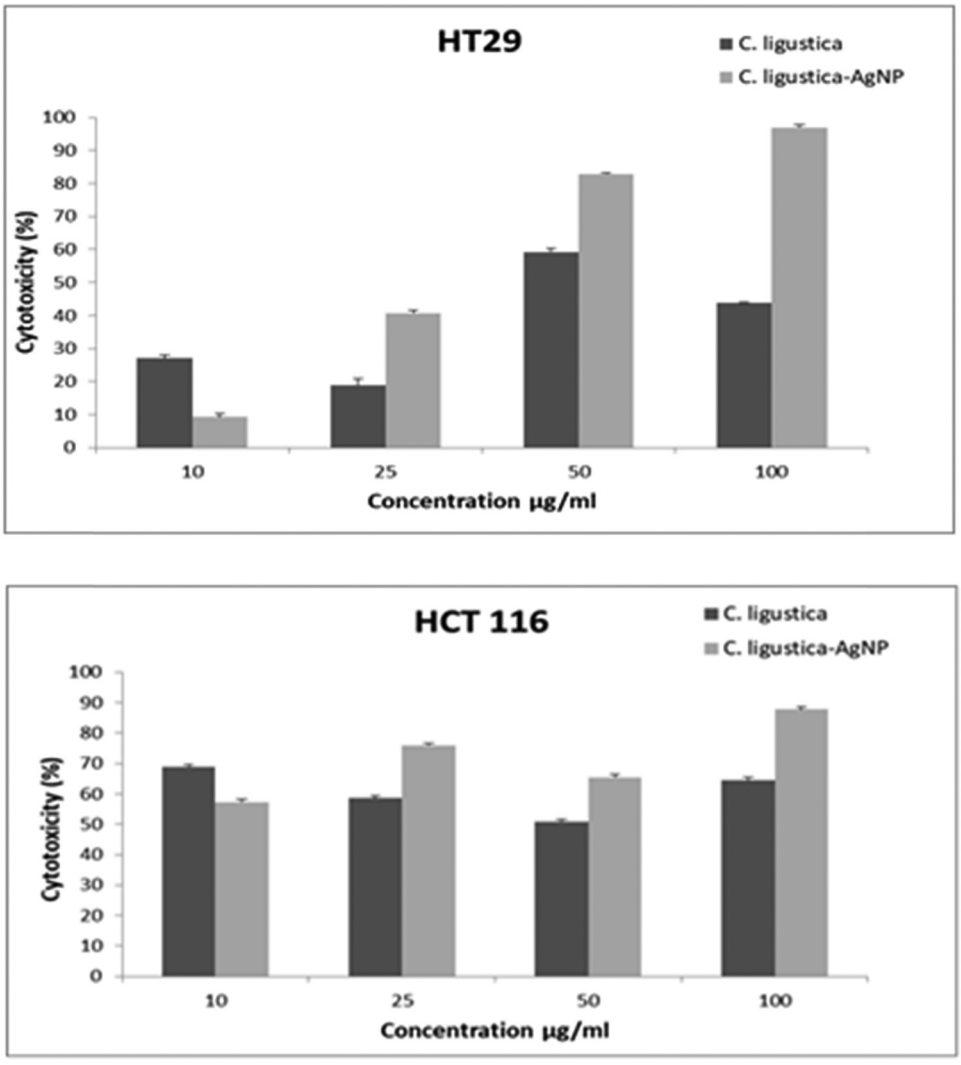

Figure 4: Cytotoxicity of *C. ligustica* extract and *C. ligustica* AgNPs against human colon cancer cell lines HT29 and HCT116.

involved in the green synthesis of nanoparticles from metal ions [30,31]. *C. ligustica* extract was found rich in active metabolites (Figure 1) as shown by IR spectrum peaks, which may have supported the green synthesis process of AgNPs [15]. Our results suggested that compounds with hydroxyl, alkene, carboxyl, and amide groups of the protein, polysaccharides, and phenols present in *C. ligustica* extract were likely involved in the synthesis process as some peak shifts were seen in *C. ligustica* AgNPs spectral at 2369.98 specific for O–H stretch (carboxylic acids), C–H stretch (alkenes); 1749.29 specific for N–H bend (nitro compounds, amides), C–C stretch (amides); and 1373.36 specific for S (=O) 2 stretch (sulfones), N–O stretch (nitro compounds), O–H bend (carboxylic acids, alcohols), which are mainly assigned for proteins, polysaccharides, and polyphenols. Our results are in agreement with some earlier findings showing hydroxyl and carbonyl groups of algal biomass as reducing and capping agents for the successful synthesis of metal nanoparticles [32].

4.2 GC-MS analysis of *C. ligustica* extracts

C. ligustica extract showed antitumor properties against both the cell lines, which shows its potential as an antitumor drug. The GC-MS profile of the *C. ligustica* extracts showed the presence of some anticancer compounds. Fucoxanthin is reported to induce G1 cell-cycle arrest and apoptosis in various cancer cell lines and in animal models of cancer [33]. Eucalyptol is an active anticancer compound that induces cell death through reactive oxygen species-mediated apoptosis [34,35]. Propanoic acid, milbemycin B, and rhodopin detected in *C. ligustica* extract are achieving a lot of interest due to their cytotoxic properties

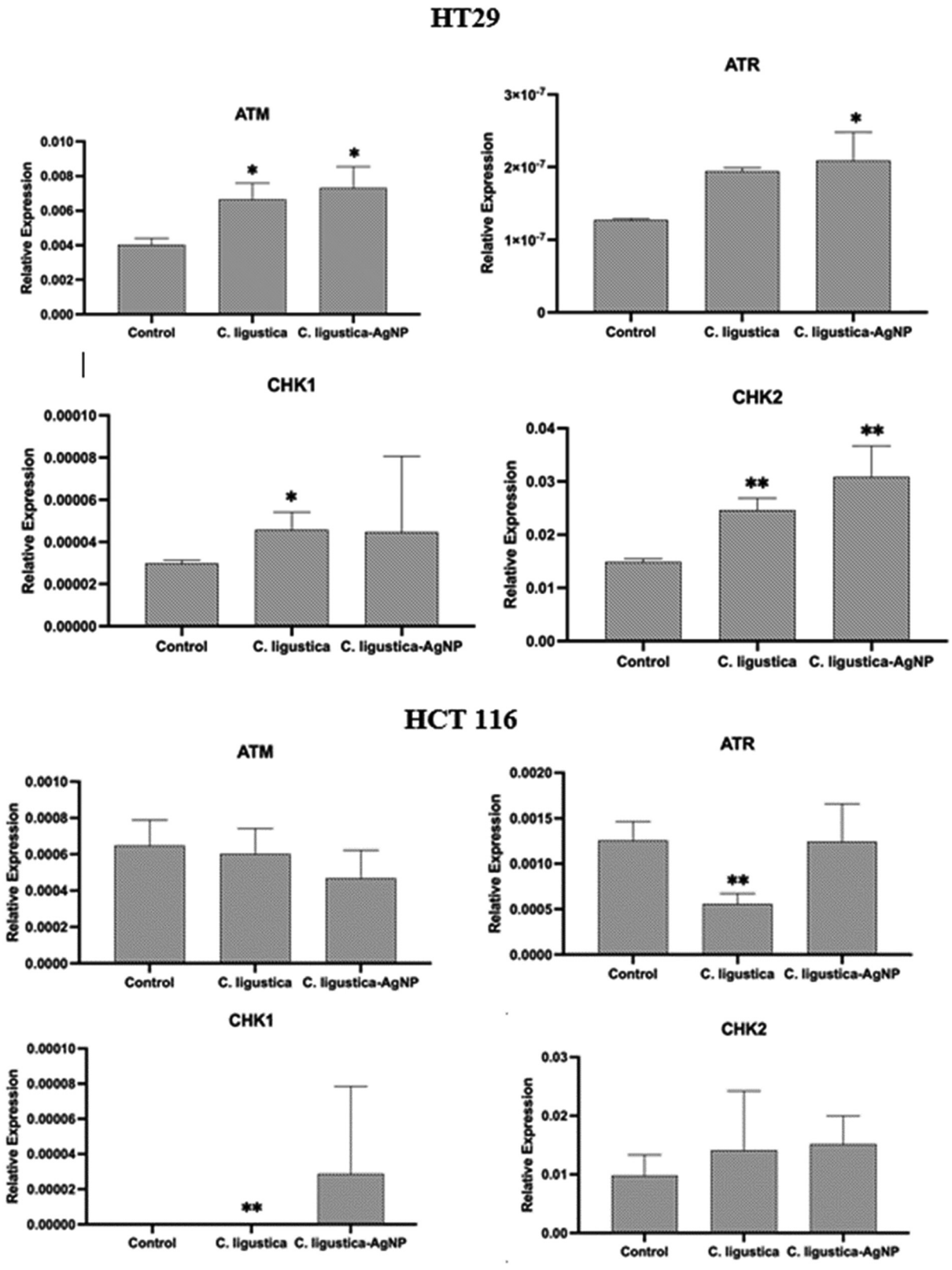

Figure 5: Gene expression fold change in cell lines treated with *C. ligustica* extract and *C. ligustica* AgNPs.

against various cancer cell lines [36–38]. Several biochemical and microscopic experiments revealed the anticancer potential of methanone [39].

4.3 Characterization of *C. ligustica* AgNPs

AgNPs were successfully synthesized from C. *ligustica* extract. It is well known that the formation of AgNPs is initially confirmed by recording a sharp surface plasmon resonance (SPR) in the range from 350 to 500 nm; however, the position of the peak is decided by the shape and size of the nanoparticle formed [40,41]. The absorption peak at 420 nm (Figure 3a) confirms SPR in AgNPs [41]. These results confirm the particle size below 100 nm with a small degree of polydispersity, which is in agreement with our zetasizer and TEM results. Overall, the size of the nanoparticle was satisfactory as the polydispersity index was 0.013, indicating little aggregation. The TEM is a perfect tool to study the morphology of particles at the nanoscale [42]. Our TEM images were clearly showing spherical shapes with particle sizes in the range from 2 to 12 nm.

4.4 Cell viability

Both *C. ligustica* extract and its biogenic AgNPs showed cytotoxicity against cancer cell lines in a dose-dependent manner, but nanoparticles were found to be more toxic than the algae extract. Our results generally agree with many studies that highlight the efficacy of AgNPs against different types of cancer cell lines [26,27]. HT29 was found to be more sensitive than HCT116. Our results are well supported by Gurunathan et al. [28] reporting plant-based nanoparticles are more effective against HCT116 as compared to HT29.

4.5 Expressional level of ATM, ATR, CHK1, and CHK2 in cell lines treated with *C. ligustica* extract and *C. ligustica* AgNPs extract

We analyzed the gene expression of ATM, ATR, CHK1, and CHK2 in both the cell lines after treating the cells with C. *ligustica* extract and its biogenic AgNPs. All these genes are involved in DNA damage response and cell cycle checkpoints. The gene expression of ATM was significantly increased in HT29 but slightly decreased in HCT116 after treatment. The ATM gene expression is considered a predictive biomarker in colorectal cancer. Decreased expression levels of ATM are associated with poor survival in colon cancer patients [43]. The loss of ATM expression is directly related to chromosomal instability and worse survival in colorectal cancer associated [44]. The expression level of ATR, CHK1, and CHK2 was significantly increased in both cell lines, but it was more prominent in HT29. All cell lines have their unique characteristics depending on the origin from tumor tissue samples of a patient [45,46]. HT29 is derived from a female adenocarcinoma-primary, whereas HCT116 is derived from male carcinoma-primary [47]. HT29 has a deficient *p53* gene expression, but HCT116 has mutations in *PI3KCA* and *K-RAS* genes [48]. Recent report by Khorrami et al. states that biogenic nanoparticles can interrupt the metabolic pathway of cancer cells even at the very lowest concentration [49].

5 Conclusion

To the best of our knowledge, bio-reduction of silver ions by *C. ligustica* aqueous extract has been reported for the first time. The produced AgNPs show peak at 420 nm in the UV-Vis spectra; TEM images showed particle size in the range from 2 to 12 nm. Quick formation of AgNPs in presence of *C. ligustica* extract showed the presence of active metabolites, which was confirmed by FTIR and GC-MS analyses. GC-MS profile showed some anticancer compounds in *C. ligustica* extracts. *C. ligustica* and its biogenic nanoparticles have good potential to be explored for anticancer compounds. *C. ligustica* and its biosynthesized AgNPs hold huge potential for pharmaceuticals mainly for cancer therapies.

Acknowledgements: The author would like to thank Deanship of Scientific Research in King Saud University for funding and supporting this research through the initiative of DSR Graduate Students Research Support (GSR).

Funding information: Deanship of Scientific Research in King Saud University funded and supported this research through the initiative of DSR Graduate Students Research Support (GSR).

Author contributions: Ramesa Shafi Bhat: writing – original draft, writing – review and editing; Sabah Ahmed Al-Zahra, Sarah A. Al Rashed, Amer Mahmood, Ahmed Al Fahad, Ghadah Alamro, and Jamilah Almusallam: methodology; Roua Al Subki and Raha Orfali: resources;

Sooad Al Daihan: project administration, resources, writing – review and editing.

Conflict of interest: Authors state no conflict of interest.

References

[1] Tugume P, Nyakoojo C. Ethno-pharmacological survey of herbal remedies used in the treatment of paediatric diseases in Buhunga parish, Rukungiri District, Uganda. BMC Complement Altern Med. 2019;19:353. doi: 10.1186/s12906-019-2763-6.

[2] Al Shehri SD, Abdul Hameed RM, Taha AZ, Almusalmi AM, Almulaify MS, Alkhabbaz FL. Complementary and alternative medicine practice and perceptions of attendees of primary care centers in Eastern Saudi Arabia. J Family Community Med. 2020;27(2):120–4. doi: 10.4103/jfcm.JFCM_218_19.

[3] Rawla P, Sunkara T, Barsouk A. Epidemiology of colorectal cancer: incidence, mortality, survival, and risk factors. Prz Gastroenterol. 2019;14(2):89–103. doi: 10.5114/pg.2018.81072.

[4] Sheikh I, Sharma V, Tuli HS, Aggarwal D, Sankhyan A, Vyas P, et al. Cancer chemoprevention by flavonoids, dietary polyphenols and terpenoids. Biointerface Res Appl Chem. 2020;11:8502–37.

[5] Vasas G. Microalgae as the source of natural products. Orv Hetil. 2018 May;159(18):703–8. doi: 10.1556/650.2018.30956.

[6] Pradhan B, Nayak R, Patra S, Jit BP, Ragusa A, Jena M. Bioactive metabolites from marine algae as potent pharmacophores against oxidative stress-associated human diseases: a comprehensive review. Molecules. 2020;26(1):37. doi: 10.3390/molecules26010037.

[7] Senthilkumar K, Manivasagan P, Venkatesan J, Kim SK. Brown seaweed fucoidan: Biological activity and apoptosis, growth signaling mechanism in cancer. Int J Biol Macromol. 2013;60:366–74.

[8] Newman DJ, Cragg GM. Marine-sourced anti-cancer and cancer pain control agents in clinical and late preclinical development. Mar Drugs. 2014;12:255–78.

[9] Murphy C, Hotchkiss S, Worthington J, McKeown S. The potential of seaweed as a source of drugs for use in cancer chemotherapy. J Appl Phycol. 2014;26:1–54.

[10] Kwak JY. Fucoidan as a marine anticancer agent in preclinical development. Mar Drugs. 2014;12:851–70.

[11] Varshney A, Singh V. Effects of algal compounds on cancer cell line. J Exp Biol. 2013;1:337–52.

[12] Ferdous UT, Yusof ZNB. Medicinal prospects of antioxidants from algal sources in cancer therapy. Front Pharmacol. 2021;12:593116. doi: 10.3389/fphar.2021.593116.

[13] Jiang J, Shi S. Seaweeds and cancer prevention. Bioactive Seaweeds for Food Applications. Academic Press, Elsevier Inc.; 2018. p. 269–90.

[14] Rocha DHA, Seca AML, Pinto DCGA. Seaweed secondary metabolites in vitro and in vivo anticancer activity. Mar Drugs. 2018;16:410.

[15] Salehi B, Sharifi-Rad J, Seca AML, Pinto DCGA, Michalak I, Trincone A, et al. Current trends on seaweeds: looking at chemical composition, phytopharmacology, and cosmetic applications. Molecules. 2019;24(22):4182. doi: 10.3390/molecules24224182.

[16] Chaudhary R, Nawaz K, Khan AK, Hano C, Abbasi BH, Anjum S. An overview of the algae-mediated biosynthesis of nanoparticles and their biomedical applications. Biomolecules. 2020;10(11):1498. doi: 10.3390/biom10111498.

[17] Heinemann MG, Rosa CH, Rosa GR, Dias D. Biogenic synthesis of gold and silver nanoparticles used in environmental applications: a review, Trends Environ Anal Chem. 2021;30:e00129.

[18] Naikoo GA, Mustaqeem M, Hassan IU, Awan T, Arshad F, Salim H, et al. Bioinspired and green synthesis of nanoparticles from plant extracts with antiviral and antimicrobial properties: a critical review, J Saudi Chem Soc. 2021;25(9):101304.

[19] Raju D, Mehta UJ, Ahmad A. Simple recovery of intracellular gold nanoparticles from peanut seedling roots. J Nanosci Nanotechnol. 2015;15:1575–81.

[20] Ali MA, Ahmed T, Wu W, Hossain A, Hafeez R, Islam Masum MM, et al. Advancements in plant and microbe-based synthesis of metallic nanoparticles and their antimicrobial activity against plant pathogens. Nanomaterials (Basel). 2020;10(6):1146.

[21] Ramos AP, Cruz MAE, Tovani CB, Ciancaglini P. Biomedical applications of nanotechnology. Biophys Rev. 2017 9(2):79–89.

[22] Saravanan M, Vahidi H, Medina Cruz D, Vernet-Crua A, Mostafavi E, Stelmach R, et al. Emerging antineoplastic biogenic gold nanomaterials for breast cancer therapeutics: a systematic review. Int J Nanomed. 2020;19(15):3577–95.

[23] Saravanan M, Barabadi H, Vahidi H, Webster TJ, Medina-Cruz D, Mostafavi E, et al. Emerging theranostic silver and gold nanobiomaterials for breast cancer: present status and future prospects, Handbook on nanobiomaterials for therapeutics and diagnostic applications. Vol. 19. Elsevier B.V.; 2021. p. 439–56.

[24] Abd El-Hack ME, Abdelnour S, Alagawany M, Abdo M, Sakr MA, Khafaga AF, et al. Microalgae in modern cancer therapy: current knowledge. Biomed Pharmacother. 2019;111:42–50.

[25] Moussavou G, Kwak DH, Obiang-Obonou BW, Maranguy CA, Dinzouna-Boutamba SD, Lee DH, et al. Anticancer effects of different seaweeds on human colon and breast cancers. Mar Drugs. 2014;12(9):4898–911. doi: 10.3390/md12094898.

[26] Daghestani M, Al Rashed SA, Bukhari W, Al-Ojayan B, Ibrahim EM, Al-Qahtani AM et al. Bactericidal and cytotoxic properties of green synthesized nanosilver using *Rosmarinus officinalis* leaves. Green Process Synth. 2020;9:230–6.

[27] Ratan ZA, Haidere MF, Nurunnabi M, Shahriar SM, Ahammad AJS, Shim YY, et al. Green chemistry synthesis of silver nanoparticles and their potential anticancer effects. Cancers (Basel). 2020;12(4):855. doi: 10.3390/cancers12040855.

[28] Gurunathan S, Qasim M, Park C, Yoo H, Kim JH, Hong K. Cytotoxic potential and molecular pathway analysis of silver nanoparticles in human colon cancer cells HCT116. Int J Mol Sci. 2018;19(8):2269.

[29] Sathishkumar RS, Sundaramanickam A, Srinath R, Ramesh T, Saranya K, Meena M, et al., Green synthesis of silver nanoparticles by bloom forming marine microalgae *Trichodesmium erythraeum* and its applications in antioxidant, drug-resistant bacteria, and cytotoxicity activity. J Saudi Chem Soc. 2019;23(8):1180–91.

[30] Grace CE, Lakshmi PK, Meenakshi S, Vaidyanathan S, Srisudha S, Mary MB. Biomoleculartransitions and lipid accumulation in green microalgae monitored by FTIR and Raman analysis. Spectrochimica Acta A Mol Biomol Spectrosc. 2020;224:117382.
[31] Marslin G, Siram K, Maqbool Q, Selvakesavan RK, Kruszka D, Kachlicki P, et al. Secondary metabolites in the green synthesis of metallic nanoparticles. Materials (Basel). 2018;11(6):940.
[32] Chugh D, Viswamalya VS, Das B. Green synthesis of silver nanoparticles with algae and the importance of capping agents in the process. J Genet Eng Biotechnol. 2021;19:126.
[33] Satomi Y. Antitumor and cancer-preventative function of fucoxanthin: a marine carotenoid. Anticancer Res. 2017;37(4):1557–62. doi: 10.21873/anticanres.11484.
[34] Boukhatem MN, Sudha T, Darwish NHE, Chader H, Belkadi A, Rajabi M, et al. A new eucalyptol-rich lavender (*Lavandula stoechas* L.) essential oil: emerging potential for therapy against inflammation and cancer. Molecules. 2020;25(16):3671. doi: 10.3390/molecules25163671.
[35] Sampath S, Veeramani V, Krishnakumar GS, Sivalingam U, Madurai SL, Chellan R. Evaluation of in vitro anticancer activity of 1,8-Cineole-containing n-hexane extract of *Callistemon citrinus* (Curtis) Skeels plant and its apoptotic potential. Biomed Pharmacother. 2017;93:296–307. doi: 10.1016/j.biopha.2017.06.056.
[36] Li X, Jiang Z, Feng J, Zhang X, Wu J, Chen W. 2-Acetylamino-3-[4-(2-acetylamino-2-carboxyethylsulfanylcarbonylamino) phenyl carbamoylsulfanyl] propionic acid, a glutathione reductase inhibitor, induces G2/M cell cycle arrest through generation of thiol oxidative stress in human esophageal cancer cells. Oncotarget. 2017;8(37):61846–60. doi: 10.18632/oncotarget.18705.
[37] Faith-Anthony AO, Ibrahim N, Hamzah A. Clinical potentials of bacteriocarotenoids: Rhodopin and β-carotene from phototrophic *Rhodopseudomonas palustris*. IOSR J Dental Med Sci. 2014;13(12):52–58.
[38] Li XQ, Yue CW, Xu WH, Lü YH, Huang YJ, Tian P, et al. A milbemycin compound isolated from Streptomyces Sp. FJS31-2 with cytotoxicity and reversal of cisplatin resistance activity in A549/DDP cells, Biomed Pharmacotherapy. 2020;128:110322.
[39] Islam K, Pal K, Debnath U, Sidick Basha R, Khan AT, Jana K, et al. Anti-cancer potential of (1,2-dihydronaphtho[2,1-b] furan-2-yl) methanone derivatives. Bioorg Med Chem Lett. 2020;30(20):127476. doi: 10.1016/j.bmcl.2020.127476.
[40] Ider M, Abderrafi K, Eddahbi A, Ouaskit S, Kassiba A. Silver metallic nanoparticles with surface plasmon resonance: synthesis and characterizations. J Clust Sci 2017;28:1051–69.
[41] Ashkarran AA, Bayat A. Surface plasmon resonance of metal nanostructures as a complementary technique for microscopic size measurement. Int Nano Lett 2013;3:50.
[42] Eskandari MJ, Gostariani R, Asadabad MA. Transmission electron microscopy of nanomaterials. In: Electron Crystallography. UK: Intech Open; 2020. p. 9.
[43] Morio T, Ku KH. Artemis and ataxia-telangiectasia-mutated: signaling networks in DNA damage. Int J Biochem Cell Biol. 2008;4(40):598–603.
[44] Beggs AD, Domingo E, McGregor M, Presz M, Johnstone E, Midgley R, et al. Loss of expression of the double strand break repair protein ATM is associated with worse prognosis in colorectal cancer and loss of Ku70 expression is associated with CIN. Oncotarget 2012;3:11.
[45] Kodack DP, Farago AF, Dastur A, Held MA, Dardaei L, Friboulet L, et al. Primary patient-derived cancer cells and their potential for personalized cancer patient care. Cell Rep. 2017;21(11):3298–309.
[46] Salvadores M, Fuster-Tormo F, Supek F. Matching cell lines with cancer type and subtype of origin via mutational, epigenomic, and transcriptomic patterns. Sci Adv. 2020;6(27):eaba1862.
[47] Davidson D, Coulombe Y, Martinez Marignac V, Amrein L, Grenier J, Hodkinson K, et al. Irinotecan and DNA PKcs inhibitors synergize in killing of colon cancer cells. Invest N Drugs. 2012;30(3):1248–56.
[48] Wang J, Kuropatwinski K, Hauser J, Ross MR, Zhou Y, Conway A, et al. Colon carcinoma cells harboring PIK3CA mutations display resistance to growth factor deprivation induced apoptosis. Mol Cancer Ther. 2007;6(3):1143–50.
[49] Khorrami S, Kamali F, Zarrabi A. Bacteriostatic activity of aquatic extract of black peel pomegranate and silver nanoparticles biosynthesized by using the extract. Biocat Agric Biotech. 2020;25:101620.